International Journal of Applied Mechanics
Vol. 1, No. 4 (2009) 557–568

ICP Imperial College Press
www.icpress.co.uk

STRAIN DECONCENTRATION IN THIN FILMS PATTERNED WITH CIRCULAR HOLES

MATTHEW B. TUCKER and TENG LI*

Department of Mechanical Engineering, Maryland NanoCenter
University of Maryland, College Park, MD 20742, USA
**LiT@umd.edu*

Received 14 June 2009
Accepted 28 July 2009

It is well known that a circular hole in a blanket thin film causes strain concentration near the hole edge when the thin film is under tension. The increased strain level can be as high as three times of the applied tension. Interestingly, we show that, by suitably patterning an array of circular holes in a thin film, the resulting strain in the patterned film can be decreased to only a fraction of the applied tension, even at the hole edges. The strain deconcentration in the film originates from the following deformation mechanism: while initially planar, the film patterned with circular holes elongates by deflecting out of plane, so that a large tension induces only small strains. Using finite element simulations, we investigate the effects of geometric parameters (i.e., hole size, spacing, and pattern) and loading direction on the resulting strain in patterned thin films under tension. The large deformability of the patterned film is independent of materials and length scale, and thus sheds light on a potential architecture concept for flexible electronics.

Keywords: Thin films; deformability; flexible electronics; patterning.

1. Introduction

In recent years, there has been a surge of interest in flexible electronics. Potential applications of flexible electronics include paper-like displays, skin-like smart prosthesis, and printable thin-film solar cells, to name a few [Dennler and Sariciftci, 2005; Forrest, 2004; Rogers and Bao, 2002; Someya *et al.*, 2004; Wagner *et al.*, 2004]. Flexible electronics in service are subject to large, repeated deformation (stretches, bends and twists). Thin films of electronic materials (e.g., metals, Si, SiO_2, etc.), however, are stiff and often fracture at small strains (e.g., $\sim$1%) [Alaca *et al.*, 2002; Chiu *et al.*, 1994; Gleskova *et al.*, 1999; Huang and Spaepen, 2000; Li *et al.*, 2004]. How to achieve large, reliable deformability of thin stiff films of electronic materials remains as a grand challenge for the success of flexible electronics technology. This paper shows that a thin film patterned with an array of circular holes can sustain large tensile deformation due to strain deconcentration. These results illustrate a general structural concept to enhance the deformability of thin stiff films.

*Corresponding author.

Recent research efforts have led to several concepts to improve the deformability of thin stiff films. In an island concept enabling stretchable electronic surfaces, thin device islands of a stiff material (e.g., SiN) are fabricated on a compliant polymer substrate [Bhattacharya *et al.*, 2005; Hsu *et al.*, 2004; Lacour *et al.*, 2006b]. When the whole structure is stretched, the deformation is mainly accommodated by the polymer substrate, and the induced strain in the majority part of a stiff island is small. The resulting strain near the island edges, however, can be significant and may cause island cracking if the island size exceeds a critical value (e.g., a few hundred microns).

In a pre-stretch concept, a thin stiff film is deposited on a rubber-like substrate that is pre-stretched. Upon release of the pre-stretch, a wavy surface pattern forms due to the film wrinkling under the substrate contraction [Choi *et al.*, 2007; Khang *et al.*, 2006; Lacour *et al.*, 2003]. Such wavy structures can then be stretched up to the pre-stretch strain, by flattening the film wrinkles. By controlling the wrinkling shape of the film via controlled interfacial adhesion, uniaxial deformability up to 100 percent can be achieved [Sun *et al.*, 2006].

Figure 1 illustrates a general principle to achieve large deformability of thin films of stiff materials by suitable in-plane patterning [Li *et al.*, 2005]. A piece of paper is cut into a serpentine, and pulled at the two ends. While initially planar, the serpentine elongates by deflecting out of plane, so that a large elongation induces only small strains. Simulations show that the maximum strain in the serpentine is ∼1% at an elongation of 25%. By contrast, a straight paper stripe breaks at an elongation of only several percent. This general principle is also demonstrated by recent experiments of thin gold films (25 nm thick) on elastomeric substrates (1 mm thick) [Lacour *et al.*, 2006a]. The surface of the as-fabricated gold film is covered with tri-branched microcracks randomly distributed throughout the film. The gold ligaments that demarcate the cracks, however, form a network that percolates the whole film. Such thin gold films on elastomeric substrates can sustain repeated elongation of 32% for more than 100 cycles, without appreciable fracture

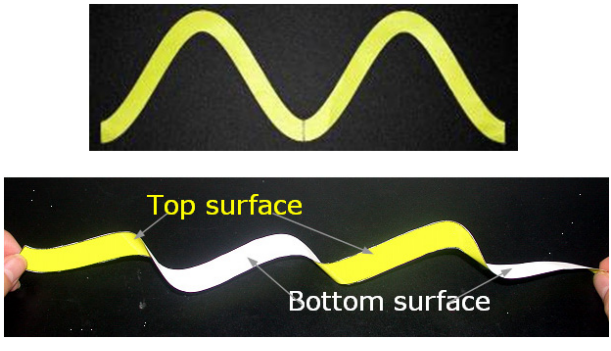

Fig. 1. An initially planar paper serpentine elongates by deflecting out of plane. The resulting strain in the serpentine is small even though the overall elongation is large.

and fatigue. Further simulations show that the gold ligaments deflect out of plane to accommodate the large elongation. As a result, majority part of the gold film undergoes elastic deformation even though the overall elongation is large. The above two examples demonstrate that the general principle of achieving large deformability of thin stiff films by suitably patterning is essentially geometric, thus independent of materials and length scales. Therefore, it is further proposed that such a deformable thin stiff film can serve as a platform, on which the whole integrated circuit can be fabricated. The resulting architecture can sustain large, repeated deformation without device materials fracture.

While the serpentine patterns and tri-branched microcrack patterns enable enhanced deformability of thin stiff films, these patterns also suffer from their shortcomings. The serpentine films have limited surface areas. Therefore, if used as the platform for the whole circuit, the number of circuit components (e.g., transistors) that can be integrated on such films is limited. Moreover, serpentine films have rather limited biaxial deformability. While a network of serpentines has biaxial deformability, such a network pattern is difficult to fabricate due to the sharp corners and the possible self-avoiding issues. The tri-branched microcracks in the abovementioned gold films are formed spontaneously during the film deposition on elastomeric substrates, and thus are randomly distributed. Mandlik *et al.* [2006] recently fabricated thin gold films with pyramidal features in a geometric pattern on elastomeric substrates. Such patterned thin gold films can sustain elongations of up to 25% in certain directions while remaining electrically conductive. The enhanced deformability of the gold films is attributed to the pyramids that impede crack propagation in the gold films. The fabrication of such pyramidal features in thin gold films involves multiple lithographical steps, thus is not suitable for high output manufacture.

In fact, a large variety of patterns allows substantial elongation of thin stiff films by the abovementioned general principle. In this paper, we investigate the deformability of thin stiff films patterned with an array of circular holes. Such patterns are planar, thus can be easily fabricated with two-dimensional microfabrication techniques. The resulting patterned stiff films have biaxial deformability and connectivity. Recent experiments demonstrated that, a thin gold film (75 nm thick) patterned with circular holes (about 5 um in diameter) on an elastomeric substrate (250 um thick) can sustain elongations of 30% [Wagner and Jones, 2008]. Under such a large elongation, microcracks appear near the edge of some holes but the majority part of the film remains intact. In contrast, a continuous thin gold film of same thickness on a same substrate suffers from cracking all over the film when subject to such a large elongation. These preliminary experimental results demonstrate the large deformability of thin stiff films patterned with circular holes. So far, however, quantitative understanding of the parameters that govern the deformability of the patterned thin films (e.g., hole geometry and distribution, tensile directions, and film/substrate relative stiffness etc.) remains elusive.

To address the above issues and plan further systematic experiments, the rest of the paper is organized as follows. Section 2 discusses why patterned circular holes in a thin stiff film lead to strain deconcentration, rather than cause strain concentration near the hole edges. Using finite element simulations, Sec. 3 studies the effects of hole size, hole spacing and loading directions on the resulting strain in a thin stiff film with circular holes patterned in a triangle lattice and subject to uniaxial elongation. These results are then compared with those for a thin stiff film with circular holes patterned in a square lattice in Sec. 4. Further discussions on the driving force for crack growth in the patterned thin films are given in Sec. 5.

2. Strain Concentration Vs. Strain Deconcentration

It is well known that a circular hole in a thin blanket film results in strain concentration near the hole edge when the film is under tension. The overall elongation of the film is accommodated by pure *in-plane stretch*. The strain level near the circular hole can be as high as three times of the applied tensile strain (Fig. 2(a)). The strain concentration near the hole becomes more significant if the hole assumes an elliptic shape. For a thin film with a sharp crack, the limiting case of an ellipse, the strain at the crack tip tends to infinity when such a film is under a finite tension.

In contrast, for a thin film patterned with an array of circular holes, the film ligaments that demarcate the circular holes form a network of hidden serpentines

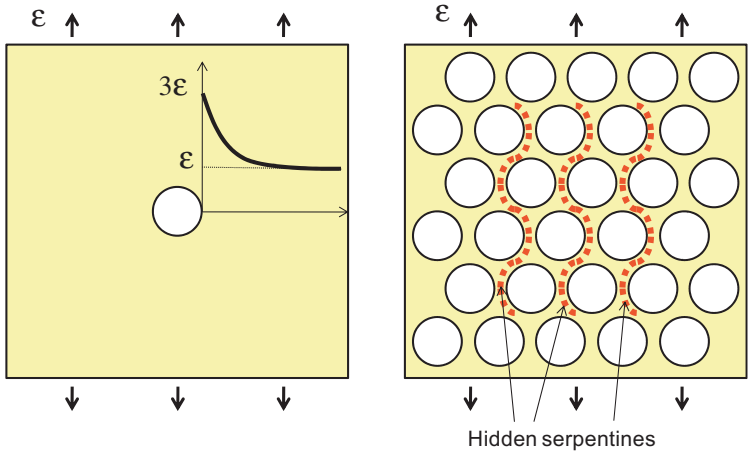

(a) (b)

Fig. 2. (a) Under tension, a blanket thin film with a circular hole stretches *in the plane*, leading to strain concentration near the hole edge up to three times of the applied tension. The strain concentration decays at locations away from the hole edge. (b) In a thin film patterned with an array of circular holes, the film ligaments that demarcate the holes form hidden serpentines (e.g., dotted curves). Such serpentines deflect *out of plane* when the film elongate. As a result, the strain in the film is deconcentrated, even near the hole edges.

(Fig. 2(b)). When such a film is subject to tension, these hidden serpentines can *deflect out of plane* to accommodate the overall elongation (e.g., to be shown in Fig. 4(a)). The resulting strain due to deflection scales with the ratio between thin film thickness and radius of curvature of the deformed film. Under a modest elongation, the radius of curvature of the deformed film is comparable with the feature size of the pattern (e.g., spacing between holes), which is often much larger than the thin film thickness. Consequently, the resulting strain in the film can be significantly deconcentrated, compared to the highly concentrated strain when the film stretches in the plane. For example, as will be shown later, the maximum strain in the film patterned with circular holes can be as low as only half of the applied tension.

It has been shown that the strain deconcentration in a serpentine under tension (e.g., Fig. 1) becomes more substantial if the ratio between the amplitude and the pitch of the serpentine increases (i.e., a more tortuous serpentine) [Li *et al.*, 2005]. Similarly, for the film with patterned circular holes under tension, the strain deconcentration becomes more substantial if the circular holes are more densely packed (i.e., more tortuous hidden serpentines). It is also expected that the pattern distribution and the tensile direction also influence the strain deconcentration in the film.

In practice, patterning a thin stiff film with in-plane features needs to be carried out on the surface of a substrate. The mechanical interaction between the patterned thin stiff film and the underlying substrate strongly influences the deformation behavior of the thin film. If the substrate is too stiff, the film deformation is mainly confined in the plane of substrate surface. As a result, the overall elongation is accommodated by the in-plane stretch, leading to large strains in the film. If the substrate is sufficiently compliant, its surface can be pulled up or pressed down, following the out-of-plane deformation of the thin stiff film. For example, recent simulations show that, under tension, a patterned thin gold film on an elastomeric substrate deforms almost like a freestanding thin gold film with the same pattern [Li *et al.*, 2005].

In the next two sections we quantify the effects of pattern geometry, loading direction and substrate stiffness on the strain deconcentration of thin films patterned with circular holes.

3. Thin Stiff Films with Circular Holes Patterned in a Triangle Lattice

3.1. *Simulation model*

Figure 3(a) illustrates a thin stiff film of thickness t patterned with circular holes of radius R, whose centers coincide with a triangle lattice of lattice spacing L. Due to the symmetry of the pattern, we only simulate a shaded area of the patterned thin film. We study the deformation of the shaded area under tensions in two different directions as defined in Fig. 3(a). Given the symmetry of the triangle lattice, these

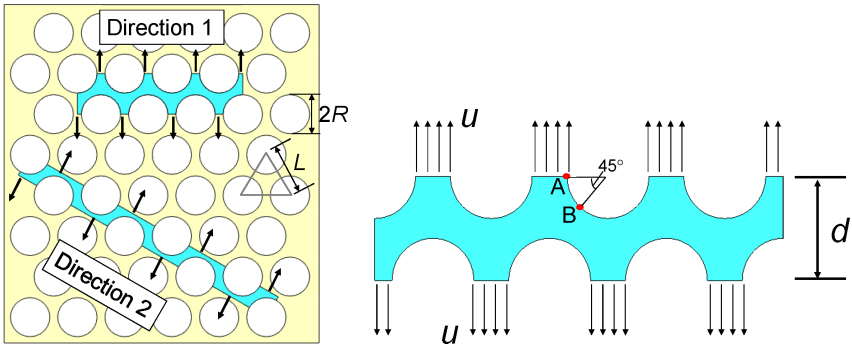

(a) (b)

Fig. 3. (a) A thin film patterned with circular holes whose centers coincide with a triangle lattice. The two shaded areas illustrate the simulation models under two representative tensile directions, respectively. (b) Schematic of the simulation model.

two directions represent the limiting cases of all possible tensile directions. The film ligaments along the two long parallel sides of the shaded area are subject to displacement u (Fig. 3(b)). To avoid confusion with the microscopic strain in the film, we call the quantity $2u/d$ the relative elongation of the film, where d is the width of the shaded area. The simulation is conducted using the finite element code ABAQUS. The shaded area is meshed with three-node triangle shell elements with about 100 elements along one semi-circle hole edge and size-matching elements everywhere. We model the film as a linear elastic material, with Young's modulus $E = 100\,\text{GPa}$ and Poisson's ratio $\nu = 0.3$. In simulations, $L/t = 100$, $R/L = 0.25$, 0.35 and 0.45.

To study the effect of substrate stiffness, we simulate two deformation modes of the patterned thin stiff film under tension: pure in-plane stretch and out-of-plane deflection. These two deformation modes represent two limiting cases: a patterned thin stiff film on an extremely stiff substrate, and a patterned thin stiff film on a sufficiently compliant substrate, respectively. The deformability of such a patterned thin stiff film on a substrate of finite stiffness is expected to be in between the predicted deformability of these two limiting cases. To allow the out-of-plane deflection in the initially planar thin film, an imperfection of small amplitude, obtained from a buckling eigen-mode analysis, is introduced to perturb the deformation of the shaded area. The uniaxial elongation of the patterned film leads to bi-axial stress state in the film due to lateral contraction. Elastomers often have larger Poisson's ratios (∼0.5) than those of the stiff electronic materials (∼0.3). When a patterned stiff film on a compliant elastomer substrate is subject to uniaxial tension, the elastomer substrate tends to contract more in the lateral direction than the stiff film, imposing extra lateral compression to the pattern film. However, due to the huge film/substrate stiffness ratio in such a case, the contribution to the bi-axial

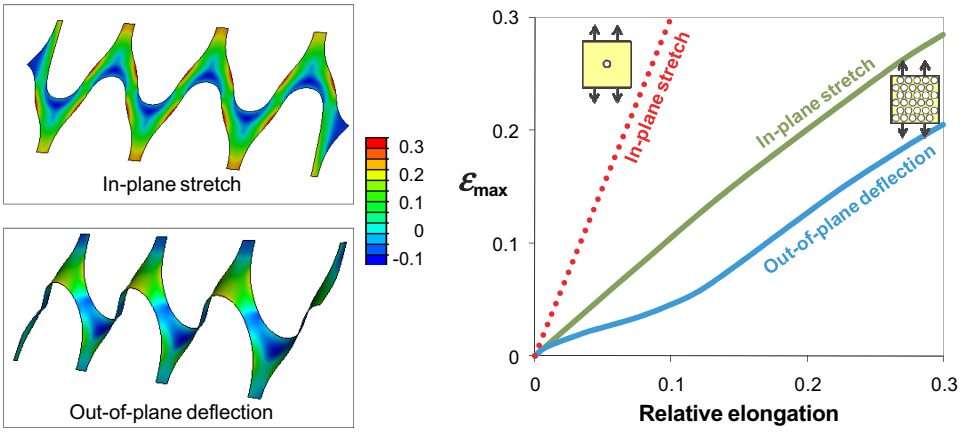

(a) (b)

Fig. 4. (a) Deformed shapes of the shaded area in Fig. 3(b) under a relative elongation of 30%, for two deformation modes. Note the difference in the strain level in the film, as indicated by the color shades. (b) The maximum principal strain $\varepsilon_{\max}$ in the film as a function of relative elongation. For a blanket thin film with a single circular hole, $\varepsilon_{\max}$ is three times of the relative elongation. For a thin film patterned with an array of circular holes, in-plane stretch of the film leads to $\varepsilon_{\max}$ comparable to the relative elongation, while out-of-plane deflection of the film further deconcentrates the strain to only a fraction of the relative elongation.

stress state of the stiff film due to the Poisson's ratio mismatch is of secondary significance.

3.2. *Results*

Figure 4(a) shows the deformed shapes of the shaded area ($R/L = 0.45$) at a relative elongation of 30%. At each point in the film, the strain has two principal components, the larger of which is indicated by the shade in Fig. 4(a). If the deformation of the film is confined in the plane, the resulting strain can be as large as the applied elongation in certain locations near the hole edges. Note that such a strain level in the patterned film is already deconcentrated by about three-fold, compared to that in a thin blanket film with a single circular hole subject to the same elongation. Furthermore, if the patterned thin film deforms out of plane to accommodate the elongation, the resulting strain can be further deconcentrated. For example, at the relative elongation of 30%, the strain in majority part of the film is below 10%, with a maximum value of about 20%.

Figure 4(b) further plots the maximum principal strain in the film, $\varepsilon_{\max}$, as a function of relative elongation, for both in-plane stretch mode and out-of-plane deflection mode. If the film deformation is confined in the plane (i.e., on a rigid substrate), $\varepsilon_{\max}$ is comparable to the applied elongation, with a roughly linear dependence. If the film can deflect out of plane (i.e., on a sufficiently compliant substrate), $\varepsilon_{\max}$ is only a fraction of the applied elongation. For example, at a

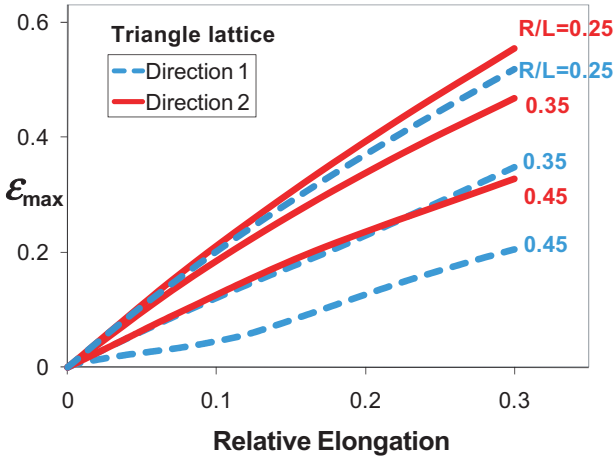

Fig. 5. $\varepsilon_{\max}$ in a thin film with circular holes patterned in a triangle lattice as a function of relative elongation, for various R/L ratios and two representative tensile directions.

relative elongation of 10%, $\varepsilon_{\max}$ is only 4%, and majority part of the film experiences less than 2% tensile strain.

To further quantify the effect of circular hole geometry and tensile direction on the strain deconcentration in the film due to out-of-plane deflection, Fig. 5 plots the maximum principal strain $\varepsilon_{\max}$ as a function of relative elongation, for various circular hole size/spacing ratios R/L and under uniaxial tensions in the two directions defined in Fig. 3(a). In all cases, $\varepsilon_{\max}$ increases monotonically as relative elongation increases. For a given relative elongation in a given tensile direction, the larger the circular hole size/spacing ratio R/L, the smaller $\varepsilon_{\max}$. The more substantial strain deconcentration results from the more tortuous hidden serpentines in a film with more densely packed circular holes. Furthermore, the maximum strain in the film under tension in direction 1 is smaller than that in the film under tension in direction 2, with all other parameters remain the same. For a given R/L, the $\varepsilon_{\max}$ vs. relative elongation curves for tensile directions 1 and 2 define the lower and upper limits of the curves for all other possible tensile directions.

4. Thin Stiff Films with Circular Holes Patterned in a Square Lattice

Figure 6(a) illustrates a thin stiff film of thickness t patterned with circular holes of radius R, whose centers coincide with a square lattice of lattice spacing L. The simulation models are shown as the shaded areas. We study the resulting strains due to out-of-plane deflection when the film is under tension in two different directions as defined in Fig. 6(a), respectively. The element type, meshing scheme and material properties used in the finite element models are the same as those defined in Sec. 3. In simulations, $L/t = 100$, $R/L = 0.25$, 0.35 and 0.45.

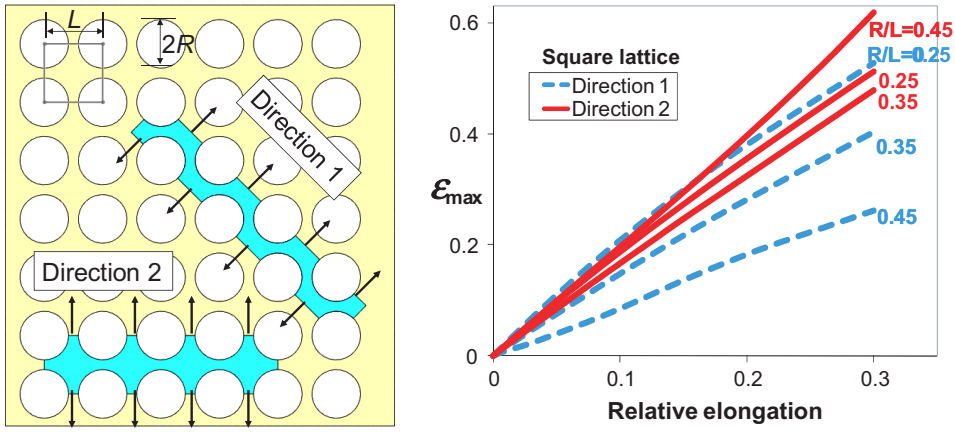

(a) (b)

Fig. 6. (a) A thin film patterned with circular holes whose centers coincide with a square lattice. The two shaded areas illustrate the simulation models under two representative tensile directions, respectively. (b) $\varepsilon_{\max}$ as a function of relative elongation, for various R/L ratios and two representative tensile directions.

Figure 6(b) plots the maximum principal strain $\varepsilon_{\max}$ as a function of relative elongation, for various values of R/L and two tensile directions. In all cases, $\varepsilon_{\max}$ increases monotonically as relative elongation increases. Under a given relative elongation in direction 1, $\varepsilon_{\max}$ decreases as R/L increases. Under a given relative elongation in direction 2, $\varepsilon_{\max}$ decreases as R/L increases in a modest range (e.g., $R/L < 0.35$), but increases if R/L is rather large (e.g., $R/L = 0.45$). The increased strain level in a film with a large R/L value under tension in direction 2 can be explained as follows. As shown in the shaded area in Fig. 6(a), there is no hidden serpentine along the tensile direction 2. Therefore, the elongation is accommodated by the pure stretch of the film ligaments that demarcate the circular holes. The pure stretch concentrates near the thinnest segment of the ligaments (e.g., all edges along the two long parallel sides in the shaded area of direction 2), resulting in strain higher than the applied elongation.

5. Discussion

In our models, we assume the edges of the circular holes are smooth and free of defects. In practice, microfabrication procedures during film patterning inevitably introduce defects near the hole edges, such as missing grains, sharp corners, etc. When the film is subject to tension, these defects can initiate cracking in the film. Crack growth eventually leads to the failure of the whole film. In recent tensile experiments of thin gold films patterned with circular holes on elastomeric substrates, microcracks appear near the edge of some holes but majority part of the film remains intact [Wagner and Jones, 2008]. To further understand why such

patterned thin gold films can sustain large elongation without crack growth, we perform the following simulations.

A microcrack is introduced at the edge of a circular hole. Two representative locations and orientations of the microcrack are considered: a microcrack perpendicular to the tensile direction at point A marked in Fig. 3(b), and a microcrack oriented 45° from the tensile direction at point B marked in Fig. 3(b). Here we consider a thin film patterned with circular holes in triangle lattice and with $R/L = 0.45$, under two deformation modes: in-plane stretch and out-of-plane deflection, respectively.

Figure 7 plots the energy release rate G at the microcrack tip, normalized by ER, as a function of relative elongation. The quantity G/ER measures the driving force for crack growth. Once G reaches a critical value G_c, the microcrack grows. The larger the relative (macroscopic) elongation of the film, the larger the driving force for crack growth. Figure 7 reveals that, if the film can deflect out of plane, the energy release rate at the microcrack tip is much smaller than that due to in-plane stretch. For example, at a relative elongation of 20%, the energy release rate at a 45° crack tip due to out-of-plane deflection is only one-seventh of that due to in-plane stretch. For a thin metal film of thickness t, G_c scales with σ_Y and t, where σ_Y is the yield strength of the metal. With $\sigma_Y = 1\,\text{GPa}$, $t = 100\,\text{nm}$, $E = 100\,\text{GPa}$, and $R = 4.5\,\mu\text{m}$, we have $G_c/ER = 2.2 \times 10^{-4}$. With such a critical value, the maximum relative elongation without microcrack growth is well beyond 30% if the metal film can deflect out of plane. In contrast, if the film deformation is confined in the plane, the maximum relative elongations are only 18% and 25% to prevent microcrack growth at the two representative locations A and B, respectively.

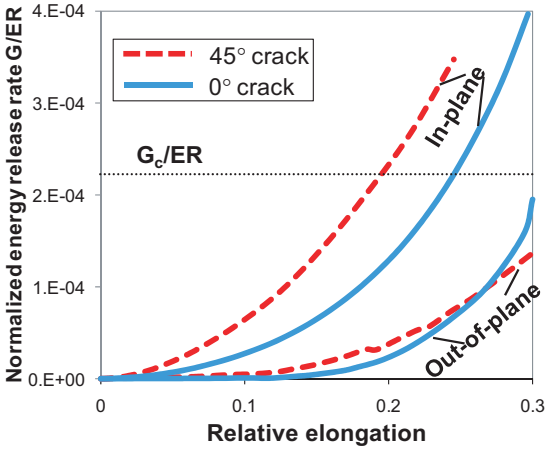

Fig. 7. Normalized energy release rate G/ER at the microcrack tip as a function of relative elongation. Note the significant difference in the driving force of crack growth for the two deformation modes. G_c denotes the threshold value above which the microcrack grows under monotonic loading.

G_c estimates the threshold of crack growth under monotonic elongation. Under cyclic loading, the fatigue crack growth threshold G_{th} is not well understood for thin metal films, but nonetheless is a fraction of G_c [Suresh, 1998]. From Fig. 7, for $G_{th} = G_c/10$, a film patterned with circular holes can still be cyclically elongated up to 16.5% without crack growth if it can deform out of plane.

6. Concluding Remarks

In this paper, we study the deconcentrated strain in thin stiff films patterned with circular holes under large elongation. We show that a suitably patterned film can elongate by deflecting out of plane. Consequently, large elongations induce small strains in the film. Using finite element simulations, we quantify the effects of pattern geometry, loading direction and substrate stiffness on the strain deconcentration in these patterned films. The calculation of the driving force for crack growth near the hole edges further explains the large deformability of the patterned thin stiff films demonstrated in recent experiments. The quantitative results from this paper (e.g., Figs. 5, 6(b) and 7) can serve as guidelines in designing flexible thin films patterned with circular holes to satisfy certain deformability criterion.

Furthermore, the general principle of achieving large deformability of thin stiff films by suitably patterning (e.g., circular holes) is essentially geometric, thus independent of materials and length scales. Therefore, such a structural principle can be potentially applied at both device and component levels in designing architecture of flexible electronics. We therefore call for further experimental demonstrations of this structural principle.

Acknowledgements

This work is supported by Minta Martin Foundation and NSF CMMI-0856540. The authors thank Sigurd Wagner and Joyelle E. Jones for sharing their experimental results and helpful discussion.

References

Alaca, B. E., Saif, M. T. A. and Sehitoglu, H. [2002] *Acta Materialia* **50**, 1197–1209.

Bhattacharya, R., Wagner, S., Tung, Y. J., Esler, J. R. and Hack, M. [2005] *Proceedings of the IEEE* **93**, 1273–1280.

Chiu, S. L., Leu, J. and Ho, P. S. [1994] *Journal of Applied Physics* **76**, 5136–5142.

Choi, W. M., Song, J. Z., Khang, D. Y., Jiang, H. Q., Huang, Y. Y. and Rogers, J. A. [2007] *Nano Letters* **7**, 1655–1663.

Dennler, G. and Sariciftci, N. S. [2005] *Proceedings of the IEEE* **93**, 1429–1439.

Forrest, S. [2004] *Nature* **428**, 911–918.

Gleskova, H., Wagner, S. and Suo, Z. [1999] *Applied Physics Letters* **75**, 3011–3013.

Hsu, P. I., Huang, M., Xi, Z., Wagner, S., Suo, Z. and Sturm, J. C. [2004] *Journal of Applied Physics* **95**, 705–712.

Huang, H. B. and Spaepen, F. [2000] *Acta Materialia* **48**, 3261–3269.

Khang, D.-Y., Jiang, H., Huang, Y. and Rogers, J. [2006] *Science* **311**, 208–212.
Lacour, S., Chan, D., Wagner, S., Li, T. and Suo, Z. [2006a] *Applied Physics Letters* **88** 204103.
Lacour, S., Wagner, S., Narayan, R., Li, T. and Suo, Z. [2006b] *Journal of Applied Physics* **100** 014913.
Lacour, S. P., Wagner, S., Huang, Z. Y. and Suo, Z. [2003] *Applied Physics Letters* **82**, 2404–2406.
Li, T., Huang, Z., Suo, Z., Lacour, S. and Wagner, S. [2004] *Applied Physics Letters* **85**, 3435–3437.
Li, T., Suo, Z., Lacour, S. and Wagner, S. [2005] *Journal of Materials Research* **20**, 3274–3277.
Mandlik, P., Lacour, S. P., Li, J. W., Chou, S. Y. and Wagner, S. [2006] *IEEE Electron Device Letters* **27**, 650–652.
Rogers, J. A. and Bao, Z. [2002] *Journal of Polymer Science Part A-Polymer Chemistry* **40**, 3327–3334.
Someya, T., Sekitani, T., Iba, S., Kato, Y., Kawaguchi, H. and Sakurai, T. [2004] *Proceedings of National Academy of Science, U.S.A.* **101**, 9966–9970.
Sun, Y. G., Choi, W. M., Jiang, H. Q., Huang, Y. G. Y. and Rogers, J. A. [2006] *Nature Nanotechnology* **1**, 201–207.
Suresh, S. [1998] *Fatigue of Materials*, 2nd ed. (Cambridge University Press, Cambridge: New York).
Wagner, S. and Jones, J. E. [2008] unpublished.
Wagner, S., Lacour, S., Jones, J., Hsu, P., Sturm, J., Li, T. and Suo, Z. [2004] *Physica E — Low-Dimensional Systems & Nanostructures* **25**, 326–334.